Annealing Effects on the Physical Properties of Electrodeposited ZnO/CdSe Core−Shell Nanowire Arrays

R. Tena-Zaera,* A. Katty, S. Bastide, and C. Lévy-Clément

Institut de Chimie et Matériaux de Paris-Est, CNRS, UMR 7182, Bât. F, 2-8 rue Henri Dunant, 94320 Thiais, France

Received October 6, 2006. Revised Manuscript Received January 26, 2007

Annealing effects on the physical properties of ZnO/CdSe core−shell nanowires have been analyzed in the range of 150−400 °C. Annealing at temperatures higher than 350 °C induce a structural transition in nanocrystalline CdSe nanowire shell, from cubic zinc blende to hexagonal wurtzite structure. This transition takes place at temperatures higher than those in CdSe bulk crystals (95 °C), underlying that the CdSe structure is determined not only by the temperature but also by the crystal size. The role of free surface energy in low-dimensional CdSe systems is emphasized. Our hypothesis explains the behavior observed in CdSe nanowire shell, as well as the results from other authors in CdSe nanocrystals. Annealing at temperatures ≥350 °C also result in the increase of particle size constituting the CdSe nanowire shell from 3 nm for the as-deposited to ≥9 nm. This considerably enhances the electronic properties of the ZnO/CdSe nanowires. The improvement may result from an easier charge carrier transport in CdSe nanowire shell promoted by the loss of quantum confinement, which is revealed by optical spectroscopy. High external quantum efficiencies (>70%) in ferro-/ferricyanide solutions have been obtained for ZnO/CdSe core−shell nanowire arrays annealed at 400 °C, demonstrating their potential in nanostructured solar cells.

1. Introduction

Extremely thin absorber (*eta*)-solar cells[1] are an offshoot technology of dye-sensitized liquid-junction[2] and solid-state[3] solar cells that have been under active development during the past decade. Functioning of *eta*-solar cells is based on the solar light sensitization of nanostructured wide band gap n-type metal oxide semiconductor by an inorganic semiconductor. Among the various kinds of *eta*-solar cells,[4−7] the ZnO/CdSe/CuSCN cells based on ZnO/CdSe core−shell nanowires appear to be one of the more promising in terms of energy conversion efficiency. ZnO/CdSe nanowire arrays present an easily accessed open nanostructure which allows good infiltration of CuSCN, or eventually other hole-transporting solid material, in the remaining pore space to complete the solar cell. Nevertheless, impedance spectroscopy studies have pointed out that the charge accumulation ability in these ZnO/CdSe/CuSCN solar cells is lower than that in conventional Si ones.[8] This phenomenon, which limits their performance, has also been observed in similar nanostructured solar cells based on a TiO_2 network (TiO_2/In-$(OH)_xS_y$/PbS/PEDOT:PSS *eta*-solar cells,[5] dye-sensitized solid-state solar cells[9]) but its origin is still unknown. Therefore, despite encouraging results obtained in ZnO/CdSe/CuSCN *eta*-solar cells, fundamental characterization of ZnO/CdSe core−shell nanowires is needed to gain further insight into the mechanisms affecting the electronic properties of this nanostructure. Concurrently, methods are needed to act in a controlled manner on their physical properties, in a way that increases the solar energy conversion efficiency of final devices. In this context, thermal annealing treatments are well-suited.

This paper presents a systematic study of the physical properties of ZnO/CdSe nanowire arrays as a function of the annealing conditions. Structural, optical, and photoelectrochemical properties are emphasized, suggesting an important role of CdSe properties in the electronic performance of ZnO/CdSe nanowires. This study not only demonstrates the enhanced photovoltaic performance of ZnO/CdSe nanowire arrays due to a controlled annealing but also gives some insights about the fundamental mechanisms that promote the improvement.

2. Experimental Section

Arrays of ZnO/CdSe core−shell nanowires were obtained by a two-step electrochemical deposition process.[6] The details are given

* To whom correspondence should be addressed. Tel: +33(0)149781329. Fax: +33(0)149781203. E-mail: tena-zaera@glvt-cnrs.fr.

(1) Ernst, K.; Lux-Steiner, M. C.; Könenkamp, R. *Proceedings of the 16th European Conference On Photovoltaic Solar Energy Conversion, Glasgow*; James & James Ltd.: London, 2000; p 63.
(2) O'Regan, B.; Grätzel, M. *Nature* **1991**, *353*, 737.
(3) Bach, U.; Lupo, D.; Comte, P.; Moser, J. E.; Weissortel, F.; Salbeck, J.; Spreitzer, H.; Gratzel, M. *Nature* **1998**, *395*, 583.
(4) Ernst, K.; Belaidi, A.; Konenkamp, R. *Semicond. Sci. Technol.* **2003**, *18*, 475.
(5) Bayon, R.; Musembi, R.; Belalidi, A.; Bär, M.; Guminskaya, T.; Lux-Steiner, M. C.; Dittrich, Th. *Sol. Energy Mater. Sol. Cells* **2005**, *89*, 13.
(6) Lévy-Clément, C.; Tena-Zaera, R.; Ryan, M. A.; Katty, A.; Hodes, G. *Adv. Mater.* **2005**, *17*, 1512.
(7) Larramona, G.; Choné, C.; Jacob, A.; Sakakura, D.; Delatouche, B.; Peré, D.; Cieren, X.; Nagino, M.; Bayon, R. *Chem. Mater.* **2006**, *18*, 1688.
(8) Mora-Sero, I.; Bisquert, J.; Fabregat-Santiago, F.; Garcia-Belmonte, G.; Zoppi, G.; Durose, K.; Proskuryakov, Y.; Oja, I.; Belaidi, A.; Dittrich, Th.; Tena-Zaera, R.; Katty, A.; Lévy-Clément, C.; Barrioz, V.; Irvine, S. J. C. *Nano Lett.* **2006**, *6*, 640.
(9) Kron, G.; Egerter, T.; Werner, J. H.; Rau, W. *J. Phys. Chem. B* **2003**, *107*, 3556. Fabregat-Santiago, F.; Bisquert, J.; Palomares, E.; Durrant, J. R. *J. Appl. Phys.* **2006**, *100*, 034510.

10.1021/cm062390f CCC: $37.00
Published on Web 03/08/2007

elsewhere[6,10,11] and, also, in the Supporting Information. All arrays were deposited on commercial conducting (10 Ω/square) glass/SnO_2:F substrates, which were previously covered by a thin continuous ZnO sprayed layer.[10] As a first step, a series of ZnO nanowire arrays were electrodeposited under the same conditions. As a second step, a CdSe coating layer was electrochemically deposited[12] consecutively on all ZnO samples of the series. Each series consisted of at least 12 samples (2 for each thermal annealing condition). With respect to the reproducibility of the experiments, four series of samples were analyzed and the representative values are given in this paper.

The postdeposition thermal annealing processes were performed in an open horizontal tubular furnace in the temperature range of 150−400 °C. The samples were introduced into the furnace and removed at the annealing temperature to ensure a rapid heating and cooling of the samples.

The morphology and crystalline structure of each material were analyzed using a Leo 1530 Field Emission Scanning Electron Microscope (FE-SEM) and a Philips PW1710 powder X-ray diffractometer. The optical properties (transmission and reflectivity) were measured at room temperature with an Hitachi UV−vis−NIR 4001 spectrophotometer fitted with an integrating sphere, from 300 to 1000 nm. Photoelectrochemical (PEC) spectroscopy was carried out using a computerized home-built setup (tungsten-halogen light source, chopper, monochromator, lock-in amplifier). The samples were illuminated from the substrate side (glass side) during the experiments. The electrolyte was an alkaline solution (pH ∼ 10, adjusted by adding KOH) of 0.2 M $K_4Fe(CN)_6$ and 0.02 M $K_3Fe(CN)_6$. The external quantum efficiency (eQE) was calculated using a standard Si photodiode.

3. Results and Discussion

3.1. Morphology. The ZnO nanowire density of electrodeposited arrays is in the range of 10^9 cm^{-2} and each nanowire is 100−150 nm in diameter with a height in the range of 1−2 μm. The array surface area is roughly estimated to be enlarged by a factor of ∼10 over a flat substrate.[10,11] To sensitize the ZnO nanowires to the solar light, they were coated with a nanocrystalline CdSe layer. A conformal uniform CdSe coating was obtained, resulting in an array of ZnO/CdSe core−shell nanowires (Figure 1a,b). The nanowire shell consists of small agglomerates (∼25 nm), which collectively form a slightly open-packed structure. A CdSe shell thickness in the range of 30−40 nm was estimated from a statistical evaluation of SEM micrograph for the nanowire diameters before and after CdSe deposition.[6] The validity of this estimation is confirmed by the local CdSe thickness, which can be measured in the circled area of Figure 1b due to the accidental detachment of CdSe layer that happened occasionally when the sample was cut for SEM cross section observations.

Thus, arrays of ZnO/CdSe core−shell nanowires were obtained by a two-step electrochemical deposition. After that, they were annealed in air for 1 h at different temperatures in the range of 150−400 °C. The effects of annealing

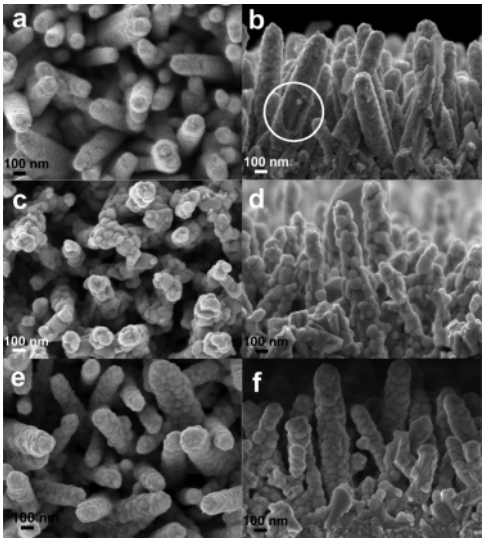

Figure 1. Scanning electron microscopy (SEM) images of ZnO/CdSe nanowire arrays after different annealing treatments: 1 h at 250 °C: (a) plan view and (b) cross section; 1 h at 400 °C : (c) plan view and (d) cross section; 1 h at 350 °C plus 1 h at 400 °C: (e) plan view and (f) cross section. In Figure 1b the circled area shows the local thickness of CdSe nanowire shell.

treatments on the physical properties of core−shell nanowire arrays were then analyzed as follows.

No relevant changes with respect to the ZnO/CdSe nanowires morphology can be observed in scanning electron microscopy (SEM) images for annealing temperatures ≤350 °C (see Supporting Information). The typical morphology is shown in Figure 1a,b (sample annealed at 250 °C), with a nanowire shell constituted by agglomerates of ∼25 nm in diameter. However, in Figure 1c,d, SEM images reveal important changes in the CdSe nanowire shell after annealing at 400 °C. The nanocrystalline layer morphology is altered into a collection of bigger oval grains, found in a wide size distribution. From a statistical analysis of the images, mean values of ∼55 and ∼95 nm are obtained for the minor and major axes, respectively. As a result of this grain growth and migration, the ZnO nanowires are not fully covered by CdSe. This can be explained in that electrodeposited CdSe volume is not large enough to maintain a continuous shell when constituted of these thicker grains. In addition, the coalescence of CdSe grains from adjacent nanowires, which were separated by ∼100 nm in as-deposited samples, also begins for annealing at 400 °C. It is interesting to note that post-annealed samples at 400 °C that had already been annealed at 350 °C result in a different CdSe layer morphology. In this case the nanowire shell maintains a continuous layer (constituted by approximately round-shaped grains of ∼50 nm in diameter) and the coalescence of grains from different nanowire shells does not take place (Figure 1e,f). Although SEM images do not reveal any particular features for samples annealed at 350 °C, this annealing induces some differences in the CdSe layer properties that play an important role during annealing at 400 °C.

The coalescence observed in Figure 1c points out that matter transport, which is a hardly expected phenomenon in completely solid systems, takes place during thermal annealing at 400 °C for as-deposited samples. This could be easily promoted by the beginning of a CdSe liquid phase

(10) Tena-Zaera, R.; Katty, A.; Bastide, S.; Lévy- Clément, C.; O'Regan, B.; Muñoz-Sanjosé, V. *Thin Solid Films* **2005**, *483*, 372.
(11) Tena-Zaera, R.; Ryan, M. A.; Katty, A.; Hodes, G.; Bastide, S.; Lévy-Clément, C. *C. R. Chim.* **2006**, *9*, 717.
(12) Cocivera, M.; Darkowski, A.; Love, B. *J. Electrochem. Soc.* **1984**, *131*, 2414.

(likely in surface), suggesting a dramatic decrease of the melting point of CdSe shell with respect to bulk material (1240 °C). A similar decrease in melting temperature was previously reported in CdS nanocrystals of 3−4 nm.[13] For small-sized nanocrystals the liquid phase is generally stabilized relative to the solid phase to minimize the surface free energy contributions.[14,15] From this point of view, annealing at 350 °C could lead to an increase of CdSe particle size that might result in higher nanowire shell melting point. The agglomerates observed by SEM (Figure 1a,b) could be constituted of small primary particles, which increase in size at 350 °C without inducing a significant change in the secondary agglomerate size (~25 nm). X-ray diffraction (XRD) has been used to confirm the presence and evolution in size of these particles.

3.2. Structural Properties. XRD measurements were made using Bragg−Brentano configuration. The data were analyzed by Rietveld refinement[16] using the Fullprof software.[17] This method presents good capabilities for the determination not only of the structural but also of the microstructural (strain and crystallite size) information. The experimental XRD peaks were fitted using the "Thompson-Cox-Hastings pseudo Voigt" function, consisting of convoluted Gaussian and Lorentzian functions.[18] With respect to peak broadening, we assumed that the Gaussian component was due to lattice distortions ("strain") and that the Lorentzian component provides information about the crystallite size, which can be estimated by Scherrer's formula (eq 1). The instrumental broadening, which was determined using a standard LaB_6 powder, was also taken into account in our calculations.

$$D_v = \frac{K_\beta \lambda}{\beta \cos \theta_B} \quad (1)$$

D_v is the volume-weighted crystallite size while K_β is a dimensionless number (1.075 for spherical crystallites),[19] λ is the X-ray wavelength, β is the integral breadth,[20] and θ is the Bragg diffraction angle.

The presence of several phases (three in the simplest case) and the very small quantity of CdSe contained in each sample complicates the refinement analysis. However, the calculated profiles were in good agreement with the measured data. A spherical geometry was considered in all cases for the crystallite size. This assumption may not be totally realistic in some cases, especially for samples annealed at 400 °C where CdSe grains show oval geometry. However, as the asymmetry is low, the calculated value should not be too far from real crystallite size. In general, the Rietveld refinement provides important clues about the structural properties of the crystallites and their evolution as a function of annealing temperature.

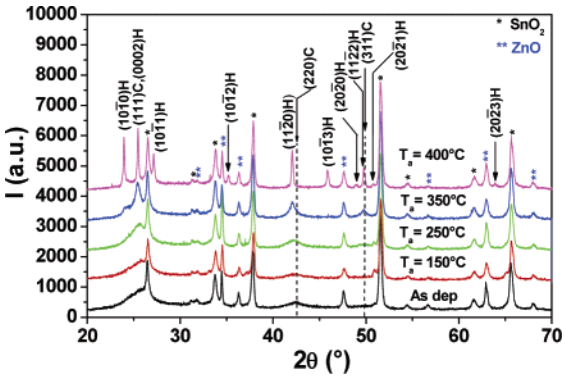

Figure 2. X-ray diffraction patterns of SnO_2/ZnO/CdSe samples annealed at different temperatures.

Table 1. Structural and Optical Properties of CdSe Nanowire Shell after Different Annealing Temperatures

	structural phase	crystallite size (nm)	optical band gap (eV)
as-deposited	ZB	3	1.88
T_a = 150 °C	ZB	3	1.86
T_a = 250 °C	ZB	4	1.77
T_a = 350 °C	ZB	9	1.73
T_a = 350 °C	WZ	9	1.73
T_a = 400 °C	WZ	>60	1.74

The experimental XRD patterns are shown in Figure 2, where the diffraction peaks from the substrate are marked with an asterisk. These peaks correspond to the SnO_2 tetragonal phase,[21] except for a small peak placed at $2\theta \sim 31.3°$. But this peak could be promoted by the presence of some $(Sn_2O_2F_4)Sn_2$ inclusions induced by high fluorine doping of SnO_2 layer.[11] With respect to the ZnO core nanowires, the diffraction peaks (labeled with two asterisks in Figure 2) can be assigned to ZnO wurtzite hexagonal structure,[22] showing the preferential orientation along the [0001] direction. No significant variations of these peaks are observed, as a function of annealing processes. This stands in contrast to the important variations in structural properties of the CdSe shell nanowires promoted by the thermal treatments and clearly reflected in the XRD measurements.

The Rietveld refinement confirmed that the cubic zinc blende (ZB) structure is the main phase of CdSe in as-deposited nanowire shells and in samples annealed below 350 °C. No clear evidence of the hexagonal wurtzite (WZ) structure of CdSe has been found under these conditions. Above 350 °C the WZ CdSe represents about 23% of the CdSe nanowire shell and becomes the main phase (and likely the sole phase) at 400 °C.

The crystallite size values obtained from eq 1 are summarized in Table 1 as a function of annealing temperature. The obtained values suggest that CdSe agglomerates observed for annealing temperatures ≤350 °C are constituted of primary nanoparticles <10 nm in diameter. If these

(13) Goldstein, A. N.; Echer, C. M.; Alivisatos, A. P. *Science* **1992**, *256*, 1425.
(14) Alivisatos, A. P. *J. Phys. Chem.* **1996**, *100*, 13226.
(15) Buffat, Ph.; Borel, J.-P. *Phys. Rev. A* **1976**, *13*, 2287. Jackson, C. L.; McKenna, G. B. *J. Chem. Phys.* **1990**, *93*, 9002. Shi, J. Q.; Shi, H. X.; Zhao, M. *J. Chem. Phys.* **1999**, *111*, 2176.
(16) Rietveld, H. M. *J. Appl. Crystallogr.* **1969**, *2*, 65.
(17) Rodriguez-Carvajal, J. Abstracts of the Satellite Meeting on Powder Diffraction of the XV Congress of the IUCr, Toulose, 1990; p 127.
(18) Thompson, P.; Cox, D. E.; Hastings, J. B. *J. Appl. Crystallogr.* **1987**, *20*, 79.
(19) Langford, J. L.; Wilson, A. J. C. *J. Appl. Crystallogr.* **1978**, *11*, 102.
(20) Laue, M. *Ann. Phys. (Leipzig)* **1936**, *26*, 55.
(21) Powder Diffraction File 00-041.-1445, PDF-2 Database Sets; International Center for Diffraction Data: Newton Square, PA, 1993.
(22) Powder Diffraction File 00-036.-1451, PDF-2 Database Sets; International Center for Diffraction Data: Newton Square, PA, 1993.

particles present some free surface, their size evolution could well explain the different 400 °C annealing effects on as-deposited samples and those already annealed at 350 °C (Figure 1c−f). The CdSe grains observed in samples annealed at 400 °C (Figure 1c,d) can be interpreted as single-crystalline domains, at least along their minor axis, as 60 nm lies in the interval of sizes deduced from SEM images. This may also be valid for samples treated by a two-step annealing (350 + 400 °C) with a crystallite size around 45 nm that is in good agreement with mean diameter (∼50 nm) estimated from SEM observations (Figure 1e,f). Concerning the CdSe phases, although ZB is considered as metastable by several authors,[23,24] it is the most frequently observed for nanocrystalline layers deposited at low temperature (T < 25 °C) by wet techniques such as chemical bath[23,25,26] and electrochemical deposition.[27−29] Moreover, its stability at low temperatures was theoretically predicted[30] and also experimentally demonstrated by Fedorov et al.[31] They reported the ZB to WZ structural transition in CdSe crystals at 95 ± 5 °C. However, our XRD data (Figure 2) in common with many other studies[23,27,32] show that nanocrystalline CdSe ZB structure is stable up to 350 °C. Hence, the crystal size appears to play an important role in ZB−CdSe stabilization.

In our case, the influence of agglomerate size on phase transformation below 350 °C does not appear to occur. However, the structural changes and growth of primary particles may be connected since both depend on the mobility of atomic species. Therefore, the size of primary particles could be the key parameter. The size of ZB crystallite increases from 3 nm in as-deposited CdSe shell nanowires to 9 nm after annealing at 350 °C. As mentioned, this temperature promotes a partial ZB to WZ structural transition, which results in WZ crystallites of the same size (9 nm). It is well-known that multiple nucleation steps promote the fractures of crystalline domains.[14] The coincidence between ZB and WZ crystallite sizes after annealing at 350 °C can be interpreted as a result of a structural transformation via a single nucleation. In this case, the possible structural defects may not play an active role in structural transition nor in the stabilization mechanisms of the ZB phase. Thus, the stability of the ZB phase should be promoted by intrinsic characteristics of CdSe nanocrystals.

Among the differences between bulk and nanocrystals, the free surface energy can be a crucial parameter due to the high surface/volume ratio in low-dimensional nanocrystals, as already shown in ZnS,[34] TiO_2,[35] or Al_2O_3.[36] For example, if spherical particles are considered, the surface/volume ratio varies as $1/r$ (r being the particle radius). Thus, although in terms of cohesion bulk energy the ZB to WZ transition should take place at ∼95 °C,[31] if the ZB surface energy is slightly lower than WZ ones, it could modify this transition temperature in small nanoparticles. In this context, the relevance of high surface energy of the cubic rock salt (RS) structure of CdSe has been noted by Alivisatos and co-workers for the WZ to RS structural transition in CdSe nanocrystals under pressure.[37] Unfortunately, the surface energy of ZB and WZ CdSe phases has not been extensively studied to our knowledge. In addition, the subtle structural differences that exist between them have not been considered in the few theoretical models that are found in the literature (e.g., ref 38). However, in the recent study reported by Erwin et al.[39] on the doping of semiconductor nanocrystals, the differences between ZB and WZ−CdSe have been taken into account to calculate the binding energy for Mn absorbates on their surfaces. The Mn−CdSe binding energy is higher for the (0001) WZ face than for its "equivalent" (111) face in ZB, indicating the relevance of the differences that exist between these two structures.

Lower free surface energies for ZB relative to WZ could compensate for the lower internal bulk energy of the latter phase in the 3−4 nm CdSe particles found in the nanowire shell annealed at temperatures ≤250 °C. However, this surface compensation contribution is not sufficient at 350 °C, as ∼23% of the particles begin to change phase. There are two possible reasons that could contribute to that. On one hand, the temperature augmentation should favor the WZ phase in terms of bulk cohesion energy. On the other hand, the increase of particle size, from 4 to 9 nm, promotes a decrease of surface/volume ratio, reducing the relevance of surface energy contributions. Thus, the ZB to WZ transition will be determined not only by the temperature but also by the crystal size. From surface energy point of view, the "particle coordination" might also be relevant. In this sense, the partial structural transition observed at 350 °C (∼23%) could take place in CdSe particles that are more closely packed with neighboring ones, i.e., present less free surface energy. Meanwhile, particles with high free surface energy, probably located in the external part of ∼25 nm agglomerates (observed by SEM), maintain the ZB phase because of a balance between surface and bulk energies.

(23) Kale, R. B.; Lokhande, C. D. *J. Phys. Chem. B* **2005**, *109*, 20288.
(24) Rivera-Márquez, A.; Rubín-Falfán, M.; Lozada-Morales, R.; Portillo-Moreno, O.; Zelaya-Angel, O.; Luyo-Alvarado, J.; Meléndez-Lira, M.; Baños, L. *Phys. Status Solidi A* **2001**, *188*, 1059.
(25) Hodes, G.; Albu-Yaron, A.; Decker, F.; Motisuke, P. *Phys. Rev. B* **1987**, *36*, 4215. Cachet, H.; Essaaidi, H.; Froment, M.; Maurin, G. *J. Electroanal. Chem.* **1995**, *396*, 175. Toyoda, T.; Tsuboya, I.; Shen, Q. *Mater. Sci. Eng. C.* **2005**, *25*, 583.
(26) Niitsoo, O.; Sarkar, S. K.; Pejoux, C.; Rühle, S.; Cahen, D.; Hodes, G. *J. Photochem. Photobiol. A* **2006**, *181*, 306.
(27) Fantini, M. C. A.; Moro, J. R.; Decker, F. *Sol. Energy Mater. Sol. Cells* **1988**, *17*, 247.
(28) Swaminathan, V.; Subramanian, V.; Murali, K. R. *Thin Solid Films* **2000**, *359*, 113. Sarangi, S. N.; Sahu, S. N. *Physica E* **2004**, *23*, 159.
(29) Hodes, G.; Grunbaum, E.; Feldman, Y.; Bastide, S.; Lévy-Clément, C. *J. Electrochem. Soc.* **2005**, *152*, G917.
(30) Yeh, C.-Y.; Lu, Z. W.; Froyen, S.; Zunger, A. *Phys Rev. B* **1992**, *46*, 10086.
(31) Fedorov, V. A.; Ganshin, V. A.; Korkishko, Y. N. *Phys. Status Solidi A* **1991**, *126*, K5.
(32) Portillo-Moreno, O.; Lozada-Morales, R.; Rubín-Falfán, M.; Pérez-Álvarez, J. A.; Zelaya-Angel, O.; Baños-López, L. *J. Phys. Chem. Solids* **2000**, *61*, 1751.
(33) Zhang, H.; Huang, F.; Gilbert, B.; Banfield, J. F. *J. Phys. Chem. B* **2003**, *107*, 13501.
(34) Zhang, H.; Banfield, J. F. *J. Mater. Chem.* **1998**, *8*, 2073.
(35) McHale, J. M.; Auroux, A.; Perrotta, J.; Navrotsky, A. *Science* **1997**, *277*, 788.
(36) Tolbert, S.; Alivisatos, A. P. *J. Chem. Phys.* **1995**, *102*, 4642. Chen, C. C.; Herhold, A. B.; Johnson, C. S.; Alivisatos, A. P. *Science* **1997**, *276*, 398.
(37) Manna, L.; Wang, L. W.; Cingolani, R.; Alivisatos, A. P. *J. Phys. Chem. B* **2005**, *109*, 6183.
(38) Erwin, S. C.; Zu, L.; Haftel, M. I.; Efros, A. L.; Kennedy, T. A.; Norris, D. J. *Nature* **2005**, *436*, 91.
(39) Bandarayake, R. J.; Wen, G. W.; Lin, J. Y.; Jiang, H. X.; Sorensen, C. M. *Appl. Phys. Lett.* **1995**, *67*, 831.

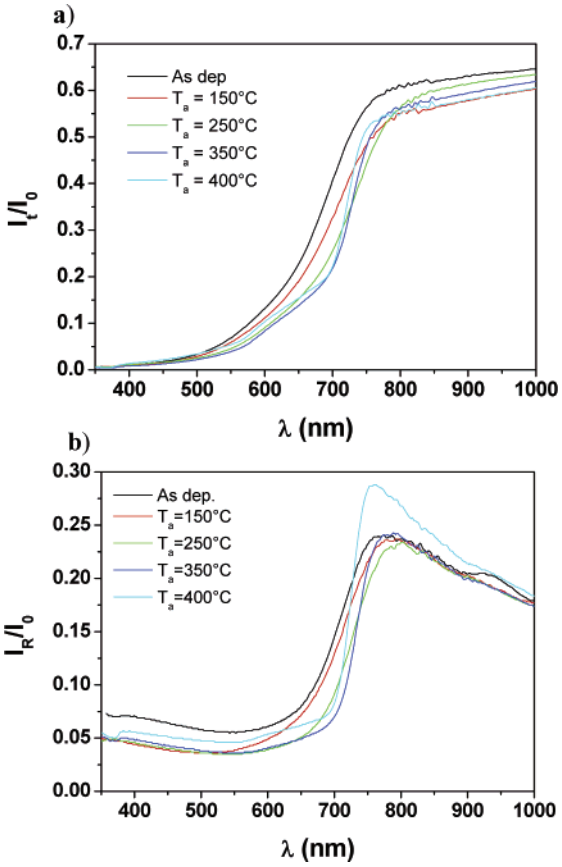

Figure 3. Optical properties: (a) transmittance and (b) reflectance of SnO_2/ZnO/CdSe samples annealed at different temperatures.

More data are necessary for the ZB and WZ surface energies to confirm our hypothesis. However, it would explain the behavior observed in our CdSe nanowire shell, as well as the results from other authors.[23,27,32,33] In addition, it points toward the tendency of small CdSe nanocrystals to exhibit the ZB phase, which is the most common case in the literature.[40] The exception is the colloidal CdSe crystals where the surface energy of WZ faces can be diminished by the presence of inorganic−organic bindings.[41]

3.3. Optical Properties. After discussing the morphology and structural properties of ZnO/CdSe nanowires, we analyze now their optical properties that are fundamental for the performance of nanostrutured solar cells. The transmittance and reflectance of samples annealed at different temperatures are shown in Figure 3.

The optical properties of ZnO core nanowires have already been studied in our previous work[10] and the analysis here is focused on the CdSe nanowire shell that absorbs the main part of incident light. Annealing treatments promote a shifted and modified optical absorption edge. The as-deposited CdSe nanowire shell shows a gradual absorption onset. Nanowires annealed at temperatures ≥350 °C result in an abrupt absorption edge and the most abrupt onset is found for samples subjected to 400 °C annealing. The position of the absorption onset was determined from the maximum derivative of the optical density (referred to optical band gap in the text). This method allows band gap estimation without knowing the effective optical thickness of the shell nanowire, considerably advantageous given our nanostructured samples that promote multiple optical reflection events. The obtained values are summarized in Table 1.

Ab initio calculations predict some slightly higher values (0.1 eV) for ZB CdSe than for WZ one.[42] This might be an explanation for the observed difference in the onset absorption position. But as both phases exhibit a direct band gap transition,[43] it cannot explain the difference in the shape of the absorption edge. In contrast, the position and shape of the absorption edge can well be understood in terms of size quantization effect. On one hand, the particle size evolution could explain the optical band gap shift as a function of the annealing temperature. The size of as-deposited CdSe particles (∼3 nm) is quite low, well below the CdSe Bohr exciton diameter (∼11 nm) promoting the charge localization that results in a blue shift of band gap relative to the bulk value (1.74 eV[44]). The blue shift diminishes as the CdSe particle size increases and is not observed for values higher than 11 nm. In our case, the lowest optical band gap value (1.73 eV) is attained after annealing at 350 °C, which results in a mixture of 9 nm ZB and WZ−CdSe nanoparticles. Similar trends have been previously reported for chemically deposited CdS and CdSe nanocrystalline layers.[32,45] The authors associated the minimum optical band gap with the structural disorder promoted by the ZB to WZ transition. Finally, after 400 °C annealing, which results in a complete structural transition and unconfined particles with a size above 11 nm (Figure 1c,d), the band gap value corresponding to bulk CdSe is found. On the other hand, the gradual absorption edge can be well understood in terms of a possible size dispersion in small particles which smears the quantum confinement effect.[46]

A quantitative analysis shows that the observed blue shift values for the confined particles are lower than those predicted by recent theoretical models[47] which introduce some improvements to the effective mass approximation (EMA), resulting in a better agreement between theoretical and experimental data for CdSe colloidal crystals.[48] Considering the crystallite sizes (Table 1) and excluding the samples annealed at ≥350 °C that present approximately the bulk band gap value, the observed shift is around 80% of the theoretically predicted value. Charge overlap interactions between neighboring particles may be the origin of this difference.[49] In fact, a total loss of quantization was reported for CdSe layer electrodeposited from a similar solution, on titanium substrates, due to a tight packing between single

(40) Didenko, Y. T.; Suslick, K. S. *J. Am. Chem. Soc*. **2005**, *127*, 12196. Zhu, J.; Palchik, O.; Chen, S.; Gedanken, A. *J. Phys. Chem. B* **2000**, *104*, 7344. Deng, Z.; Cao, L.; Tang, F.; Zou, B. *J. Phys. Chem. B* **2005**, *109*, 16671.
(41) Yin, Y.; Alivisatos, A. P. *Nature* **2005**, *437*, 664.
(42) Zakharov, O.; Rubio, A.; Blasé, X.; Cohen, M. L.; Louie, S. G. *Phys. Rev. B* **1994**, *50*, 10780.
(43) Tonmasulo, A.; Ramakrishma, M. V. *Chem. Phys*. **1996**, *210*, 55.
(44) Madelung, O. *Semiconductors Basic Data*; Springer-Verlag: Berlin, 1996.
(45) Zelaya-Angel, O.; Alvarao-Gil, J. J.; Lozadas-Morales, R.; Vargas, H.; Ferreira da Silva, A. *Appl. Phys. Lett*. **1994**, *64*, 291.
(46) Datta, S.; Narashiman, K. L. *Phys. Rev. B* **1999**, *60*, 8246.
(47) Pellegrini, G.; Mattei, G.; Mazzoldi, P. *J. Appl. Phys*. **2005**, *97*, 073706. Baskoutas, S.; Terzis, A. F. *J. Appl. Phys*. **2005**, *99*, 013708.
(48) Murray, C. B.; Norris, D. J.; Bawendi, M. G. *J. Am. Chem. Soc*. **1993**, *115*, 8706. Yu, W. W.; Qu, L.; Guo, W.; Peng, X. *Chem. Mater*. **2003**, *15*, 2854.

nanocrystals.[50] The dependence of degree of quantization as a function of electrodeposition conditions has been recently studied, finding that depositions at high current density result in greater quantum confinement.[29] Several possible reasons which could promote electronic decoupling between neighboring particles, even considering the case of direct physical contact, have been discussed in the cited paper. The structural and morphological evolution of nanowire shell in our experiments suggests a slightly open-packed nanocrystalline CdSe layer. In this context, 150 °C is probably not a sufficient thermal agitation to alter and reduce the open-packed structure, but may promote the evaporation of some residual solvent. The adsorption of these solvent traces on as-deposited CdSe nanocrystals can potentially increase the interparticle electronic decoupling, as reported for potassium cyanide.[51] Hence, solvent evaporation may result in a weak quantification loss that may explain the small decrease of the optical band gap observed after 150 °C annealing.

From the point of view of nanostructured solar cell application, reflectance values as low as possible are desired. We observe that annealing of as-deposited samples at 400 °C results in an increase of the reflectance (Figure 3b). The increased reflectance is due to the presence of agglomerates, constituted by big oval CdSe crystals at the nanowire tips (Figure 1d), that reflect the incident light before scattering by the nanowires take place, slightly diminishing the light trapping effect. However, in terms of effective absorbance (A_E),[52] this effect is compensated by the enhancement of absorbance close to the absorption edge (Figures 3a,b). High A_E values (≥80%) are obtained in the 400−800 nm range of the solar spectrum (air mass, A.M. 1.5) for all samples, irrespective of the annealing temperature.

3.4. Photoelectrochemical Properties. The ZnO/CdSe nanowire arrays show a high solar light harvesting, which was one of the limitations observed in DSSC based on ZnO nanowire arrays.[53] However, nanostructured solar cells require both high solar light absorption and efficient carrier photogeneration and injection mechanisms. To study the efficiency of the complete processes in ZnO/CdSe nanowires, PEC spectroscopy measurements were carried out in alkaline ferro-/ferricyanide solution. As can be seen in Figure 4, annealing treatments promote a red shift in eQE onset. The evolution with the annealing temperature follows the same trend as the optical absorption onset discussed above. The eQE onset values agree roughly with those of optical absorption (Figure 3a). These two observations indicate a suitable band alignment at the ZnO/CdSe interface in all cases, essential to an efficient charge carrier transfer.

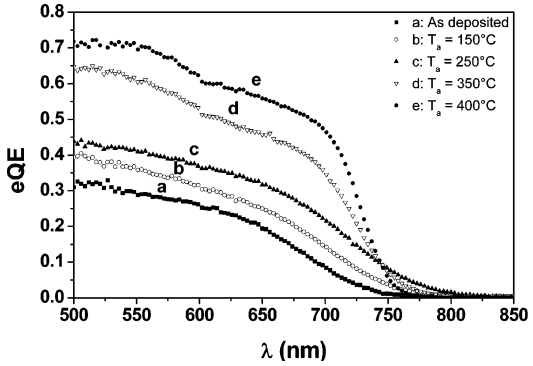

Figure 4. External quantum efficiency (eQE) of SnO_2/ZnO/CdSe samples, annealed at different temperatures, in ferro-/ferricyanide solution.

Additionally, the eQE improves with increased annealing temperature, showing the biggest variation (∼20%) between 250 and 350 °C. The highest eQE (∼72%) is attained for samples annealed at 400 °C. The abrupt increase in eQE values coincides with the total loss of quantum confinement in CdSe, as observed in optical measurements, which might facilitate the transport of charge carriers throughout a whole nanocrystalline shell nanowire. On the other hand, it also coincides with the beginning of the ZB to WZ structural transition. To that extent, Hodes et al.[54] have noted that wurtzite structure cadmium chalcogenides show longer periods of cell stability in polysulfide PEC cells. Otherwise, eQE is considerably higher for samples annealed at 400 °C (∼72%) than for those treated at 350 °C (∼65%). From the point of view of electrical transport in CdSe nanowire shell, this is not surprising because bigger CdSe crystals may increase the carrier diffusion length. However, in samples annealed directly at 400 °C CdSe grains do not fully cover the ZnO nanowire surface, inducing the contact between ZnO core nanowire and ferro-/ferricyanide electrolyte. Regarding the charge transfer at the interfaces, this may induce some recombination losses. Taking into account both considerations, a continuous CdSe nanowire shell constituted of crystals as big as its thickness seems to be the best situation. According to SEM and XRD measurements, the two-step annealing (350 + 400 °C) appears as an efficient way to obtain nanowires fulfilling these requirements. Nevertheless, at present, samples annealed by this way (Figure 1e,f) have not resulted in significant enhancements in eQE values. The dispersion in obtained eQE values was higher than the differences observed between the two different annealing ways. Larger series of samples are now under investigation to gain further insight into this point.

With respect to annealing atmosphere, Szabo and Cociviera[55] reported that the presence of oxygen during the annealing process increases the minority carrier diffusion length in thick (>1 μm) CdSe layers electrodeposited on titanium substrates, promoting a gain in QE higher than 20%. We have confirmed that samples annealed under argon result in slightly lower (∼5%) eQE values than those made under air at the same temperatures.

(49) Vossmeyer, T.; Katsikas, L.; Giersig, M.; Popovic, I. G.; Diesner, K.; Chemseddine, A.; Eychmuller, A.; Weller, H. *J. Phys. Chem.* **1994**, *98*, 7665. Artemeyev, M. V.; Bibik, A. I.; Gurinovich, L. I.; Gaponenko, S. V.; Woggon, U. *Phys. Rev. B* **1999**, *60*, 1504. Micic, O.; Ahrenkiel, S. P.; Nozik, A. J. *Appl. Phys. Lett.* **2001**, *78*, 4022.
(50) Cerdeira, F.; Torriani, I.; Motisuke, P.; Lemos, V.; Decker, F. *Appl. Phys. A: Mater. Sci. Process.* **1998**, *46*, 107.
(51) Sarkar, S. K.; Hodes, G. *J. Phys. Chem. B* **2005**, *109*, 7214.
(52) Lévy-Clément, C.; Katty, A.; Bastide, S.; Zenia, F.; Mora, I.; Munoz-Sanjosé, V. *Physica E* **2002**, *14*, 229.
(53) Law, M.; Greene, L. E.; Johnson, J. C.; Saykally, R.; Yang, P. *Nat. Mater.* **2005**, *4*, 455. Baxter, J. B.; Aydil, E. S. *Appl. Phys. Lett.* **2005**, *86*, 05311. Baxter, J. B.; Aydil, E. S *Sol. Energy Mater. Sol. Cells* **2006**, *90*, 607.
(54) Hodes, G.; Manassen, J.; Cahen, D. *J. Am. Chem. Soc.* **1980**, *102*, 5964.
(55) Szabo, J. P.; Cociviera, M. *J. Appl. Phys.* **1987**, *61*, 4820.

These data are strong evidence that the quantum efficiency in ZnO/CdSe nanowires is influenced by the CdSe primary particles size and in particular by electronic coupling between them. Although the charge carrier transport in CdSe seems to be crucial in the quantum efficiency of ZnO/CdSe nanowire arrays, the role of ZnO core nanowire should be highlighted. ZnO single-crystal nanowire arrays used as electron collectors solve the current problems related to the short effective diffusion length of electrons in porous TiO_2 network typified in analogous TiO_2/CdS/CdSe nanostructures.[26] Although ZnO nanowire arrays currently present a surface area lower than that of the TiO_2 nanocrystalline network, high solar harvesting is attained in ZnO/CdSe core−shell nanowire arrays using a CdSe layer, of 30−40 nm in thickness, as nanowire shell. The photogenerated carriers have to be transported inside CdSe layer before being transferred to the electron (or hole) collectors. To attain high quantum efficiencies, the carrier diffusion length in the absorber layer must be similar to its thickness. This is the case after annealing at 400 °C since the CdSe crystallite size approaches the thickness of nanowire shell. Thus, annealing at 400 °C, together with the particular properties of electrodeposited CdSe nanocrystalline nanowire shells (primary particle size and slightly open-packed structure), allows high external quantum efficiencies (>70%) to be obtained. This finding is an improvement from the values obtained by other recently proposed interesting inorganic nanostructures[26,56] and therefore may result in an important advance in research on nanostructured inorganic solar cells. In addition, this value is comparable to those shown by polycrystalline CdS/CdTe solar cells composed of micrometer-sized crystallites that were also made using more expensive fabrication processes.[57] By comparing recent alternatives studies, we find that inorganic nanostructures have an important new role in the frame of solar cell applications, but also that ZnO/CdSe nanowire arrays have a good position among them.

4. Conclusions

The effects of annealing conditions on the physical properties of two-step electrodeposited ZnO/CdSe core−shell nanowire arrays have been analyzed. Zinc blende structure has been found to be stable in nanocrystalline CdSe nanowire shell, until 350 °C. The free surface energy, and therefore the primary particle size, in the stabilization of this structure has been suggested to play an important role. This hypothesis may explain the structural behavior in CdSe nanowire shell, as well as the previous results in CdSe nanocrystals. The role of CdSe primary particle size has been pointed out not only in the structural properties but also in the optical and electronic behavior of ZnO/CdSe nanowire arrays. Annealing temperatures higher than 350 °C result in a CdSe nanowire shell constituted of particles ≥9 nm, considerably enhancing the electronic performance of the ZnO/CdSe nanowires. In this framework, external quantum efficiencies higher than 70% in ferro-/ferricyanide solutions have been obtained for ZnO/CdSe nanowire arrays annealed at 400 °C, demonstrating their potential in nanostructured solar cells. In conclusion, this work not only demonstrates the enhanced photovoltaic performances of ZnO/CdSe nanowire arrays due to a controlled thermal treatment but also gives some insights about the fundamental mechanisms that promote the improvements.

Supporting Information Available: Details of the two-step electrochemical process and SEM images of ZnO/CdSe nanowire arrays (as-deposited and annealed at temperatures of 150, 250, and 350 °C). This material is available free of charge via the Internet at http://pubs.acs.org.

CM062390F

(56) Robel, I.; Subramanian, V.; Kuno, M.; Kamat, P. *J. Am. Chem. Soc*. **2006**, *128*, 2385.
(57) Durose, K.; Boyle, D.; Abken, A.; Ottley, C. J.; Nollet, P.; Degrave, S.; Burgelman, M.; Wendt, R.; Beier, J.; Bonnet, D. *Phys. Status Solidi B* **2002**, *229*, 1055.